10-11-2011

A Novel Solid Oxide Redox Flow Battery for Grid Energy Storage

Nansheng Xu
University of South Carolina - Columbia, xun@cec.sc.edu

Xue Li
University of South Carolina - Columbia, lixue@cec.sc.edu

Xuan Zhao
University of South Carolina - Columbia, zhao53@cec.sc.edu

John B. Goodenough

Kevin Huang
University of South Carolina - Columbia, huang46@cec.sc.edu

Publication Info

Published in *Energy & Environmental Science*, Volume 4, Issue 12, 2011, pages 4942-4946.

Xu, N., Li, X., Zhao, X., Goodenough, J., & Huang, K. (2011). A Novel Solid Oxide Redox Flow Battery for Grid Energy Storage. Energy & Environmental Science, 4 (12), 4942 - 4946. http://dx.doi.org/10.1039/C1EE02489B

Energy & Environmental Science

Cite this: *Energy Environ. Sci.*, 2011, **4**, 4942

www.rsc.org/ees

COMMUNICATION

A novel solid oxide redox flow battery for grid energy storage†

Nansheng Xu,[a] Xue Li,[a] Xuan Zhao,[a] John B. Goodenough[b] and Kevin Huang*[a]

Received 28th August 2011, Accepted 26th September 2011
DOI: 10.1039/c1ee02489b

In this work we report proof-of-concept of a novel redox flow battery consisting of a solid oxide electrochemical cell (SOEC) integrated with a redox-cycle unit. The charge/discharge characteristics were explicitly observed by operating between fuel cell and electrolysis modes of the SOEC along with "in-battery" generation and storage of H_2 realized by an *in situ* closed-loop reversible steam-metal reaction in the redox-cycle unit. With Fe/FeO as the redox materials, the new storage battery can produce an energy capacity of 348 Wh/kg-Fe and round-trip efficiency of 91.5% over twenty stable charge/discharge cycles. This excellent performance combined with robustness, environmental friendliness and sustainability promise the new battery to be a transformational energy storage device for grid application.

Electrical energy storage plays a critical role in grid optimization of bulk power production, system balancing of variable or diurnal renewable resources, and auxiliary power services. It is the key enabler for future smart grid. Without, or with little, energy storage capability, the power grid system must rely upon redundant generation and transmission assets to meet the reliability requirements, causing significant underuse of available grid infrastructures and therefore poor system efficiency;[1–3] an unpredictable, intermittent renewable energy input from sources such as solar and wind can easily destabilize an electricity grid with varying demand, particularly with the much more dynamic utility demand of the future.[4–8]

Electrical energy storage is, in principle, a reversible energy conversion process that transforms electricity into other forms of energy (*e.g.*, kinetic, potential and chemical). Its ability to store electricity for later use makes it an ideal buffer for balancing demand and supply of electrical energy. The principal requirements for a grid-scale energy storage system include fast response time, high rate capacity, high round-trip efficiency, long cycle life, low life-cycle cost, and scalability. Of all the types of energy storage devices, redox flow battery (RFB) and Na-S/ZEBRA battery (NSB) technologies stand out with a potential to meet all of these requirements.[9–11] The more commonly known rechargeable batteries such as Li-ion are yet considered suitable for large-scale energy storage, primarily due to the concerns of safety and low rate-capacity.[12] The advantage of RFB to be flexible in system design for either power (*e.g.*, short-term frequency regulation) or energy application (*e.g.*, long-term load shifting) is a valuable asset for renewable integration. The high energy/power densities and capability to perform fast and deep charge/discharge cycles has positioned the NSB as a front runner in the commercial development of large-scale energy storage devices.

[a]*Department of Mechanical Engineering, The University of South Carolina, Columbia, SC, 29208, USA. E-mail: kevin.huang@sc.edu; Tel: +1 803-777-0204*
[b]*Department of Mechanical Engineering, The University of Texas at Austin, Austin, TX, 78713, USA*
† Electronic supplementary information (ESI) available. See DOI: 10.1039/c1ee02489b

Broader context

Successful integration of a smart grid and renewable energy sources with the existing power infrastructure depends critically upon the availability of high-performance and cost-effective energy storage. Aside from site-specific and slow-response pumped-hydro and compressed-air energy storages, development of technically advanced and economically viable large-scale electrical energy storage is still lacking. Here we demonstrate proof-of-concept of a novel redox flow battery consisting of a sold oxide electrochemical cell (SOEC) integrated with a redox-cycle unit. The charge/discharge characteristics were explicitly observed by operating between fuel cell and electrolysis modes of SOEC along with "in-battery" generation and storage of H_2 realized by *in situ* closed-loop reversible steam-metal reaction. With Fe/FeO as the redox material, the new battery can produce an energy capacity of 348 Wh/kg-Fe and round-trip efficiency of 91.5% over twenty stable charge/discharge cycles. Distinguished from conventional storage batteries, the new battery features two-electron charge-transfer electrode process and the decoupling of the structural component from the volume-changing but free-standing H_2 generation/storage unit, thus allowing it to perform simultaneous high-capacity and high-rate cycles without the concern of structural damage. These profound advantages combined with the sustainable and low-cost redox-couple materials utilized promise the new battery to be a transformational energy storage device for grid as well as other stationary applications.

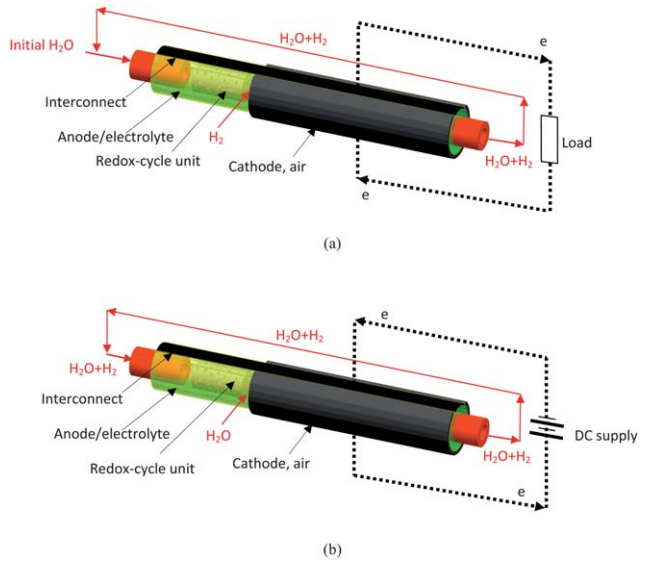

Fig. 1 Schematic of working principle of the solid oxide redox flow battery consisting of a solid oxide electrochemical cell (SOEC) of anode-supported tubular design and a redox cycle unit integrated in a closed-loop flow of steam and H_2. (a) Discharging mode; (b) Charging mode.

Despite the technological and commercial advances made in recent years, neither RFB nor NSB technology is commercially ready for the final market entry owning to the challenges they are facing.[13,14] Low energy density, short shelf life, use of toxic materials and high costs are the main factors that are hindering the commercialization of RFB technology.[8,9] The inability to sustain thermal cycling and high manufacturing cost driven by safety and by operation considerations are the impasses for NSB technology to overcome.[6,9–11] The high cost is closely related to unsatisfactory performance. Therefore, there exists a great need to develop the next-generation of advanced high-performance and low-cost storage-battery technologies for large-scale energy storage.

Here we report a new concept of storage battery consisting of a solid oxide electrochemical cell (SOEC) integrated with a redox-cycle unit, the working principle of which is illustrated in Fig.1. The SOEC is a conventional solid oxide fuel cell (SOFC) of tubular design. A thin, solid oxide-ion electrolyte (*e.g.*, YSZ) is supported by a conventional Ni-YSZ-cermet anode inner wall of the tube, and a mixed oxide-ion/electronic conductor on the outside of the tube is the cathode (Fig.S1–S2). A solid porous structure of high-surface-area Me (Me = metal) and MeO_x powder mixture as the functional redox material is installed right next to the SOEC (Fig.S3). Steam along with H_2, a product of the steam-metal reaction, flows through the SOEC and the redox-cycle unit in a closed-loop fashion (Fig.S4). Since the flow of reaction gas resembles the flow of electrode liquid in a conventional RFB, the new battery is termed "Solid Oxide Redox Flow Battery". During discharge, Fig. 1 (a), the interaction between steam and Me produces H_2 locally in the redox-cycle unit *via* the following chemical reactions

$$Me + xH_2O = MeO_x + xH_2 \quad (1)$$

The generated H_2 proceeds towards the SOEC unit operating under the fuel-cell mode by which H_2 is electrochemically oxidized at the anode, producing electricity and steam *via* the following electrochemical reactions

$$H_2 + O^{2-} = H_2O + 2e^- \quad (2)$$

When all (or a controlled utilization) the Me phase is oxidized, the discharge cycle is stopped and the battery needs to be recharged. For the charge cycle, Fig. 1(b), the high concentration of steam produced during discharge cycle is electrochemically decomposed to produce H_2 at the cathode of the SOEC unit operating under the electrolysis mode

$$H_2O + 2e^- = H_2 + O^{2-} \quad (3)$$

The generated H_2 then proceeds towards the redox cycle unit where MeO_x is chemically reduced to Me by

$$MeO_x + xH_2 = Me + xH_2O \quad (4)$$

When all (or a controlled utilization) the MeO_x is reduced to Me by H_2, the charge cycle is completed. The freshly reduced and chemically active Me is then ready for the next discharge cycle as described by reactions (1) and (2). At the air electrode, oxygen reduction and evolution take place as follows during the discharge and charge cycles

$$1/2O_2 + 2e^- \underset{\text{charge}}{\overset{\text{discharge}}{\rightleftharpoons}} O^{2-} \quad (5)$$

By combining reactions (1)–(5), the overall chemical reaction of the SORFB then becomes

$$Me + \frac{x}{2}O_2 \underset{\text{charge}}{\overset{\text{discharge}}{\rightleftharpoons}} MeO_x \quad (6)$$

In essence, reaction (6) indicates the new battery as a "metal-air" battery. Different from conventional low-temperature metal-air batteries such as Li-air and Zn-air, however, is the type of electrolyte utilized. The new battery uses a solid O^{2-}-electrolyte whereas other "metal-air" batteries use a liquid H^+-electrolyte. More electrons involved in the charge-transfer process permit the SORFB to achieve higher storage-capacity at a higher rate.

The concept of using high-temperature reversible SOFCs to produce/store H_2 with excess electricity for later generation of electricity has been previously reported.[15,16] However, this conventional approach has inherently low energy efficiency due to the external storage of large volume H_2 at high pressure and low temperature. The novelty of the new battery concept presented is the integration of an SOEC with a redox-cycle unit where H_2 can be generated and stored "*in situ*". This feature can greatly improve the overall energy efficiency of the battery.

The most profound advantage of the new battery is perhaps the separation of the structural component, *e.g.*, SOEC, from the volume-changing but free-standing H_2 generation/storage redox-cycle unit, thus allowing it to perform simultaneous high-capacity and high-rate cycles without the concern of structural damages; the latter constraint has prevented most modern storage batteries from achieving a high rate-capacity.[12]

The chief challenge facing the solid oxide redox flow battery is the variable production rate of H_2 and H_2O in the redox-cycle unit throughout charge and discharge cycles, the characteristic of which is commonly represented by an initial rapid rise to the peak rate,

followed by an exponential decay.[17–22] To mitigate such variations in concentration, the reaction gas is allowed to flow in a closed-loop during the electrical cycles. The created dynamic flow also facilitates the transport of gaseous products and reactants between the SOEC and redox-cycle unit, thus avoiding mass-transfer limitation that could be otherwise encountered in a stagnant system. The benefit from a flowing reaction gas is clearly seen by comparing Fig. 3 with Fig. S5.

The thermodynamic perspectives of the new battery are directly related to the Gibbs free energy change of reaction (6). The theoretical open circuit voltage or Nernst potential (E_N) and specific energy density (SED) of the battery using transition-metal/oxide pairs as the redox couples are shown in Fig. S8 as a function of temperature. As expected, the couples containing metals with a greater oxygen affinity exhibit higher E_N and SED because of the higher ($-\Delta G$) values. However, the performance of a storage battery also depends upon the reversibility of the metal-oxygen (or metal-steam) reaction to retain electrical cycles with high-capacity and high-efficiency. Selection of the Fe/FeO_x redox-couple in this study represents a balanced consideration of the thermodynamics and kinetics of the metal-steam reaction. The equilibrium phase composition in the Fe/FeO_x redox couple under the operating condition was first determined by the Electromotive Force (EMF) technique using SOEC as an oxygen concentration cell. Fig. 2 shows the measured EMF or Nernst potential E_N (*vs* air) as a function of H_2O content in a closed flow of two different gases, N_2–H_2O and H_2–H_2O. In the case of N_2–H_2O, $E_N = 0.970$ volt is invariant with H_2O content whereas in the case of H_2–H_2O, $E_N = 0.970$ volt only occurs above *ca.* 35% H_2O. The thermodynamic calculations predict the equilibrium partial pressure ratio of H_2 and H_2O (pH_2O/pH_2) to be 34.9/65.1 for the steam-iron reaction $Fe + H_2O = FeO + H_2$ occurring at 800 °C (Fig. S6); the $pH_2O/pH_2 = 34.9/65.1$ corresponds to an $E_N = 0.970$ volt (Fig. S7). The excellent agreement of the experimental data with the thermodynamic calculations indicates Fe and FeO as the phases prevalent in the redox material. One aspect of the new battery concept is that E_N is virtually controlled by the thermodynamic equilibrium between Fe and FeO with the actual mass ratio of Fe: FeO varying with the state of charge or discharge. The AC impedance spectra shown in Fig. 3 (a) and (b) further support the two-phase equilibrium by revealing unchanged intermediate-to-low-frequency electrode resistance above *ca.* 35% H_2O in H_2–H_2O mixture and a small systematic reduction of the intermediate-to-low-frequency electrode resistance with increasing H_2O in the N_2–H_2O mixture; latter apparently results from a reduced N_2-dilution effect while pO_2 is being fixed by the Fe–FeO equilibrium. The systematic reduction in intermediate-to-low-frequency electrode resistance below *ca.* 35% H_2O also confirms that it is an anode-related process with the lowest frequency semicircle likely being the gas diffusion process. The V–I characteristic of the battery cell measured under both fuel cell and electrolysis modes in a closed-loop flow of N_2-x%H_2O is shown in Fig. 3 (c). It is evident that the SOEC exhibited a higher resistance for electrolysis than for fuel cell in this case. Above ~57% H_2O, the cell

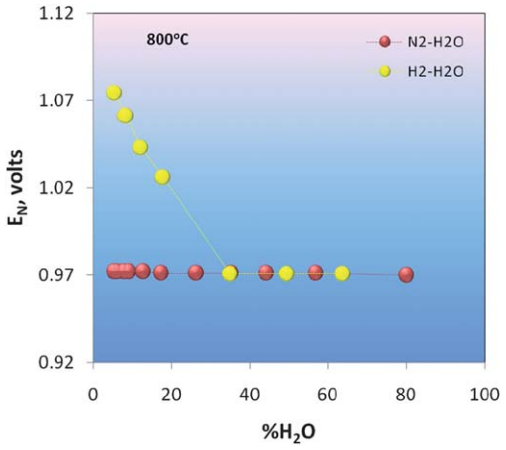

Fig. 2 Plot of E_N as a function of H_2O content in a closed-loop flow of H_2–H_2O and N_2–H_2O mixtures.

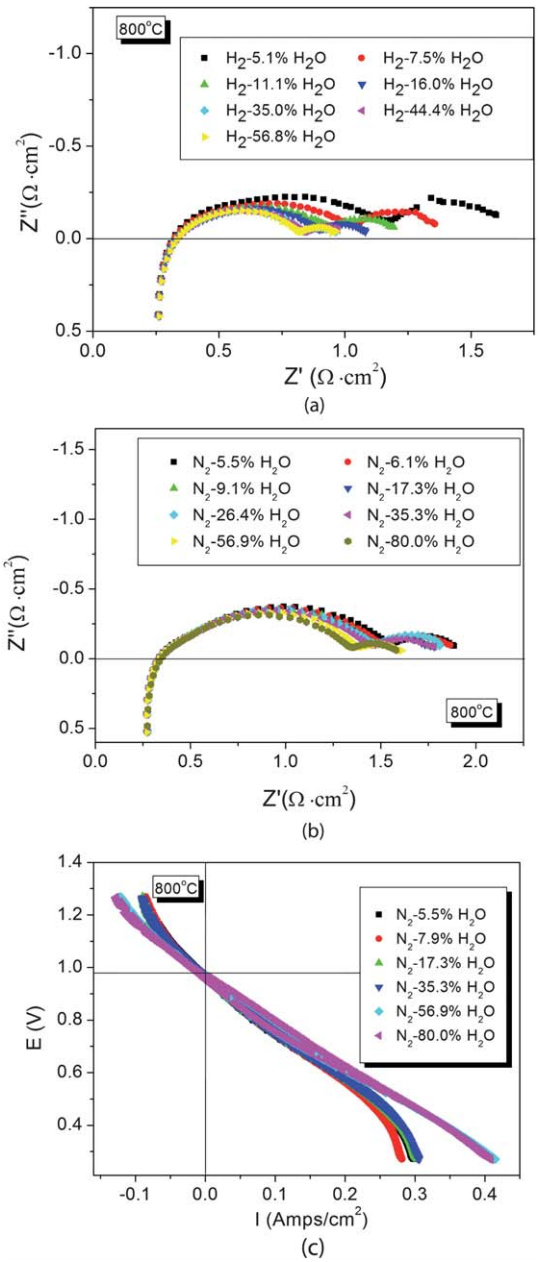

Fig. 3 AC impedance spectra of the battery measured under OCV in a closed flow of (a) H_2–H_2O and (b) N_2–H_2O. (c) V–I characteristic of the battery measured under a closed-loop flow of N_2-xH_2O.

performance is almost indiscernible. The H_2O content used in this study was ~53%, close enough to avoid significant N_2-dilution effect.

The charging/discharging characteristic of the SORFB is shown in Fig. 4 (a), where two consecutive ten charge/discharge cycles measured at a constant current density of 50 mA cm^{-2} and with a 10-minute single-cycle period are combined as one plot. The characteristic of a rechargeable battery is explicitly observed with stable performance for all the twenty cycles performed. The responses of the battery to the charge and discharge commands are instantaneous. The corresponding energy capacity calculated from integration of the voltage-time curve multiplied by the galvanic current is shown in Fig. 4 (b). The battery produces an energy density of 348 W_e h kg^{-1}-Fe averaged from the 20 electrical cycles with a 38.5% Fe utilization. This energy output is compared with the energy input during the charge cycle to yield an averaged round-trip efficiency of $\eta = 91.5\%$. Based on the capacity attained at 50 mA cm^{-2} and 38.5% Fe utilization, we can project an energy capacity of 886 W_e h kg^{-1}-Fe for 100% Fe utilization or full discharge, which comes close to about 95% of the theoretical 932 W_e h kg^{-1}-Fe (or charge capacity 960 Ah/kg-Fe). Such a close agreement favorably supports the validity of experimental data obtained. We anticipate that the charge/discharge time of the battery can be easily scaled-up to hour-level for meaningful practical applications by simply increasing the Fe loading. The rate of rechargeability (50 mA cm^{-2}) demonstrated by the SORFB is at least one order of magnitude higher than Li-ion battery (~5 mA cm^{-2}) and at a similar magnitude to RFB. However, much higher current density, *e.g.*, 300 mA cm^{-2}, is very achievable for an SOEC. The key is how to improve the performance-limiting kinetics of redox reactions occurring in the redox-cycle unit to match the SOEC performance. Investigations such as effects of microstructure and catalysts on redox-cycle kinetics,[23–26] and alternative redox materials such as high voltage and energy-density Mn/MnO couple as suggested by Fig. S8 are currently being pursued in our lab as an effort to simultaneously achieve high performance and long-term stability.[27–29] On the other hand, using SOECs with better intermediate-temperature performance, operating with pure steam at higher Fe utilization, establishing electrical performance-efficiency correlation and gaining a greater fundamental understanding of redox reactions are all good strategies to advance the solid oxide redox flow battery technology to the next level.[30–33]

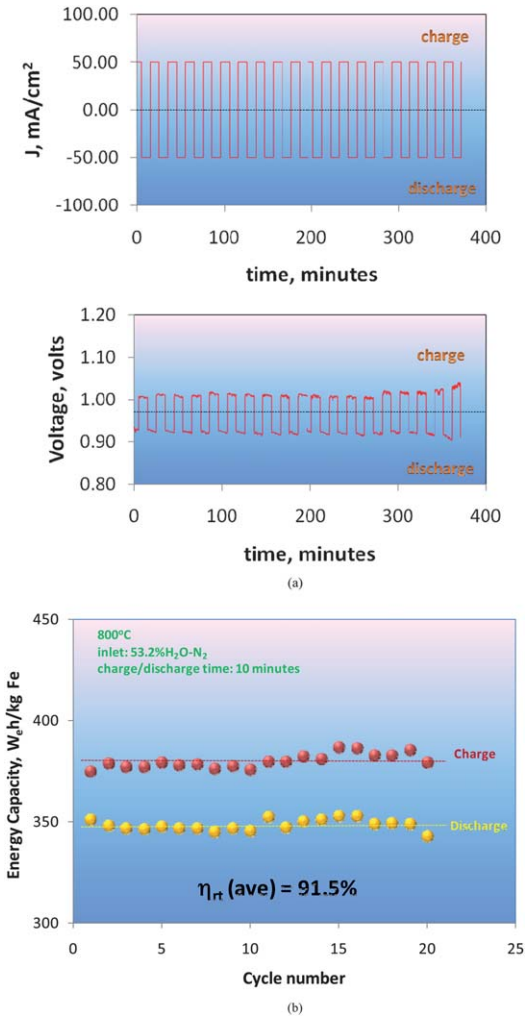

Fig. 4 (a) Charge and discharge characteristic of the battery at 800 °C and J = 50 mA cm^{-2}. The break on the curve at ~200 min marks the start of second 10-cycle run; (b) Plot of energy capacity as a function of the number of charge and discharge cycles. All data were measured with a closed-loop flow of 53.2%H_2O–N_2.

From an engineering point of view, thermal management of heat flow ($T\Delta S$ = 71.1 kJ mol^{-1} at 800 °C for reaction (6)) during exothermic discharge and endothermic charge cycles is critical to achieve a practically important thermally self-sustaining battery system. Strategies such as implementing an "in-battery" thermal storage unit to store the heat produced during the discharge cycle and release it during the charge cycle or operating the charge cycle (electrolysis) at a thermoneutral potential should be considered.[34] In addition, the efficiency calculated in this study did not consider the power loss for pumping and possible temperature variations. A more comprehensive multi-physics model taking into account all these factors can be developed in future to better estimate the system efficiency.

In summary, proof-of-concept of a novel solid oxide redox flow battery has been demonstrated in laboratory-scale tests with high storage-capacity, rate-capacity and round-trip efficiency even at relatively lower Fe loading and utilization. Its ability to store a large amount of electrical energy clearly originates from the fundamental charge/discharge reaction that essentially involves the transfer of two electrons in the electrode process. The "in-battery" generation and storage of H_2 *via* the *in situ* reversible steam-iron reaction is a thermally efficient process than conventional electrolysis/low-temperature H_2 storage approach.[15,16,35] Closed-loop circulation of the reaction gas is effective in stabilizing power and energy outputs. Most importantly, the structural component of the presented storage battery is decoupled from the volume-changing but free-standing redox-cycle unit, which gives this new battery the abilities to carry out high-rate and deep charge/discharge cycles and to sustain repeated thermal cycles without the concern of structural damage. Overall, the demonstrated performance level compares favorably with the low-temperature RFB and Na-S/ZEBRA battery technologies. These profound advantages combined with the use of low-cost and environmentally friendly redox-couple materials promise the solid oxide redox flow battery a transformational storage battery. Built on the foundation of the solid oxide electrochemical cell technology, the new battery is also anticipated to scale up at a faster pace to become a technically mature and economically viable large-scale energy storage device.

Acknowledgements

The authors acknowledge the Solid Oxide Fuel Cell Center of Excellence and Department of Mechanical Engineering in the University of South Carolina for providing seed funding to this work, Professor Ken Reifsnider for reading the manuscript with helpful suggestions and Dr Yanhai Du for supplying the anode-supported tubular solid oxide electrochemical cells. A patent application based on the presented concept and results is currently pending at the University of South Carolina (USCRF#898).

References

1 J. A. Turner, *Science*, 1999, **285**, 687.
2 M. Roeb and H. Müller-Steinhagen, *Science*, 2010, **329**, 773.
3 *Smart Grid System Report*, Office of Electricity Delivery and Energy Reliability, U.S. Department of Energy, Washington, DC, 2009.
4 N. S. Lewis, *Science*, 2007, **315**, 798.
5 D. Ginley, M. A. Green and R. Collins, *MRS Bull.*, 2011, **33**, 355.
6 D. Lindley, *Nature*, 2010, **463**, 18–20.
7 G. J. Kramer and M. Haigh, *Nature*, 2010, **463**, 293.
8 *Handbook of Energy Storage for Transmission and Distribution Applications*, Electrical Power Research Institute, Palo Alto, CA, and Department of Energy: Washington, DC, 2003.
9 Z. Yang, J. Zhang, M. C. W. Kintner-Meyer, X. Lu, D. Choi, J. P. Lemmon and J. Liu, *Chem. Rev.*, 2011, **111**, 3577–3613.
10 T. Oshima, M. Kajita and A. Okuno, *Int. J. Appl. Ceram. Technol.*, 2005, **1**, 269–276.
11 P. Poizot and F. Dolhem, *Energy Environ. Sci.*, 2011, **4**, 2003.
12 V. Etacheri, R. Marom, R. Elazari, G. Salitra and D. Aurbach, *Energy Environ. Sci.*, 2011, **4**, 3243.
13 X. Li, H. Zhang, Z. Mai, H. Zhang and I. Vankelecom, *Energy Environ. Sci.*, 2011, **4**, 1147.
14 W. Wang, S. Kim, B. Chen, Z. Nie, J. Zhang, G. Xia, L. Li and Z. Yang, *Energy Environ. Sci.*, 2011, **4**, 4068.
15 G. Tao and A. Virkar, *DOE hydrogen program annual progress report*, 2006, pp. 24–28.
16 C. Milliken, Proc. 2001 DOE hydrogen program review, NREL/CP-570–30535.
17 K. Otsuka, C. Yamada, T. Kaburagi and S. Takenaka, *Int. J. Hydrogen Energy*, 2003, **28**, 335–342.
18 E. Lorente, J. A. Peña and J. Herguido, *Int. J. Hydrogen Energy*, 2008, **33**, 615–626.
19 J. A. Peña, E. Lorente, E. Romero and J. Herguido, *Catal. Today*, 2006, **116**, 439–444.
20 V. Hacker, R. Frankhauser, G. Faleschini, H. Fuchs, K. Friedrich and M. Muhr, *J. Power Sources*, 2000, **86**, 531–535.
21 V. Hacker, *J. Power Sources*, 2003, **118**, 311–314.
22 K. Otsuka, T. Kaburagi, C. Yamada and S. Takenaka, *J. Power Sources*, 2003, **122**, 111–121.
23 S. Takenaka, T. Kaburagi, C. Yamada, K. Nomura and K. Otsuka, *J. Catal.*, 2004, **228**, 66–74.
24 K. Urasaki, N. Tanimoto, T. Hayashi, Y. Sekine, E. Kikuchi and M. Matsukata, *Appl. Catal., A*, 2005, **288**, 143–148.
25 X. Liu and H. Wang, *J. Solid State Chem.*, 2010, **183**, 1075–1082.
26 S. Takenaka, N. Hanaizumi, V. T. D. Son and K. Otsuka, *J. Catal.*, 2004, **228**, 405–6.
27 H. Wang, S. Takenaka and K. Otsuka, *Int. J. HydrogenEnergy*, 2006, **31**, 1732.
28 H. Wang, G. Wang, X. Wang and J. Bai, *J. Phys. Chem. C*, 2008, **112**, 5679.
29 V. Hacker, R. Vallant and M. Thaler, *Ind. Eng. Chem. Res.*, 2007, **46**, 8993.
30 M. C. Weinberg, D. P. Birnie III and V. A. Shneidman, *J. Non-Cryst. Solids*, 1997, **219**, 89–99.
31 M. Avrami, *J. Chem. Phys.*, 1940, **8**, 212.
32 J. Y. Park and O. Levenspiel, *Chem. Eng. Sci.*, 1975, **30**, 1207.
33 J. Y. Park and O. Levenspiel, *Chem. Eng. Sci.*, 1977, **32**, 233.
34 M. Liu, B. Yu, J. Xu and J. Chen, *J. Power Sources*, 2008, **177**, 493.
35 T. Lipman, A Clean Energy States Alliance Report, US DOE office of energy efficiency and renewable energy, Washington DC, May, 2011.

